

Reaction cycle of the yeast Isw2 chromatin remodeling complex

Daniel J Fitzgerald, Carl DeLuca, Imre Berger, Hélène Gaillard¹, Raphael Sigrist, Kyoko Schimmele and Timothy J Richmond*

ETH Zürich, Institut für Molekularbiologie und Biophysik, ETH-Hönggerberg HPK, Zürich, Switzerland

Members of the ISWI family of chromatin remodeling factors hydrolyze ATP to reposition nucleosomes along DNA. Here we show that the yeast Isw2 complex interacts with DNA in a nucleotide-dependent manner at physiological ionic strength. Isw2 efficiently binds DNA in the absence of nucleotides and in the presence of a nonhydrolyzable ATP analog. Conversely, ADP promotes the dissociation of Isw2 from DNA. In contrast, Isw2 remains bound to mononucleosomes through multiple cycles of ATP hydrolysis. Solution studies show that Isw2 undergoes nucleotide-dependent alterations in conformation not requiring ATP hydrolysis. Our results indicate that during an Isw2 remodeling reaction, hydrolysis of successive ATP molecules coincides with cycles of DNA binding, release, and rebinding involving elements of Isw2 distinct from those interacting with nucleosomes. We propose that progression of the DNA-binding site occurs while nucleosome core contacts are maintained and generates a force dissipated by disruption of histone–DNA interactions.

The EMBO Journal (2004) 23, 3836–3843. doi:10.1038/sj.emboj.7600364; Published online 9 September 2004

Subject Categories: chromatin & transcription; proteins

Keywords: chromatin remodeling; helicase proteins; Isw2

Introduction

Eukaryotic DNA is packaged into a hierarchically folded chromatin structure, which varies in density depending on its functional state and location within the genome. This organization of DNA serves to restrict access of enzymes involved in its transcription, replication, and repair to their appropriate chromosomal target sites. Eukaryotic cells locally regulate chromatin structure through two general mechanisms. One is defined by covalent modification of histone proteins that either directly influence the chromatin packaging or serve as binding sites for nuclear factors that directly alter chromatin architecture (Jenuwein and Allis, 2001). The other mechanism called chromatin remodeling is carried out

*Corresponding author. ETH Zürich, Institut für Molekularbiologie und Biophysik, ETH-Hönggerberg HPK, 8093 Zürich, Switzerland.

Tel.: +41 1 633 2470; Fax: +41 1 633 1150;

E-mail: richmond@mol.biol.ethz.ch

¹Present address: Departamento de Genética, Facultad de Biología, Universidad de Sevilla, Avenida Reina Mercedes 6, 41012 Sevilla, Spain

Received: 15 April 2004; accepted: 21 July 2004; published online: 9 September 2004

by separate families of proteins that use ATP binding and hydrolysis to drive conformational changes in local chromosome structure (Becker and Hörz, 2002).

Chromatin remodeling complexes have in common an ATP-hydrolyzing core that displays homology to members of the helicase family of proteins (Flaus and Owen-Hughes, 2001). Helicase proteins catalyze the processive separation of duplex DNA into its component single strands. These reactions consist of successive cycles of ATP hydrolysis, each of which directs a defined sequence of alterations in protein conformation (Marians, 2000). The individual nucleotide-dependent conformations have been demonstrated for numerous helicases to display differential substrate-binding activity (Wong and Lohman, 1992; Hingorani and Patel, 1993; Lohman and Bjornson, 1996; McDougal and Guarino, 2001; Majka and Burgers, 2003). To date, a reaction cycle that separately treats the component steps of an ATP hydrolysis cycle for a chromatin remodeling complex has not been described, although given the homology their ATPase domains share with those of helicase proteins, such a cycle seems likely to exist.

The yeast Isw2 chromatin remodeling complex is a member of the ISWI family of remodeling factors. ISWI-containing remodeling complexes mobilize histone octamers in *cis* along DNA in an ATP-dependent reaction. We expressed and purified the yeast Isw2 complex and investigated whether its substrate-binding properties and solution conformation change during an ATP hydrolysis cycle.

Results

A model substrate for Isw2 interaction studies

The yeast Isw2 chromatin remodeling complex was expressed in insect cells using the baculovirus system and purified to homogeneity (Figure 1A). As is the case with the endogenous complex purified from yeast (Tsukiyama *et al.*, 1999), hydrolysis of ATP into ADP and P_i is stimulated to a higher level by nucleosomes than by free DNA, and Isw2 carrying a K215R mutation in the conserved 'Walker A' motif is ATPase deficient (Figure 1B). Inclusion of the nonhydrolyzable ATP analog ATPγS in a solution containing ATP and mononucleosomes inhibited ATP hydrolysis by Isw2, suggesting that ATPγS is also accommodated in its nucleotide-binding pocket. We constructed a model mononucleosome for both remodeling and binding studies based on the '601' nucleosome positioning sequence (Thåström *et al.*, 1999; Dorigo *et al.*, 2003). 601-50 DNA comprises one 147 bp copy of the 601 nucleosome positioning sequence (Thåström *et al.*, 1999) flanked by DNA stretches of 9 and 49 bp, as based on our mapping of a nucleosome on the 601 sequence (data not shown) using our high-resolution nucleosome mapping procedure (Flaus *et al.*, 1996). This mononucleosome migrates largely as a single species on a native polyacrylamide gel (Figure 1C, lane 2). Incubation of 601-50 nucleosomes with 1 M equivalent of Isw2 results in efficient production of an

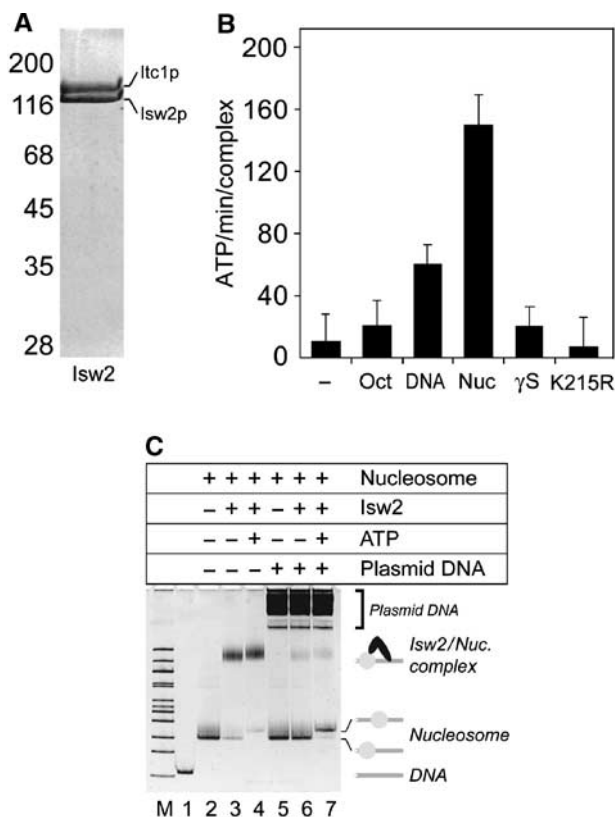


Figure 1 Recombinant Isw2 interacts with a mononucleosome model substrate. (A) Purity of the Isw2 preparation. Coomassie brilliant blue stained section of a 10% SDS gel. Isw2 comprises the Itc1p (145 kDa) and Isw2p (130 kDa) proteins. (B) Nucleosome-stimulated ATPase activity of recombinant Isw2. ATP hydrolysis rates (ATP/min/complex) are measured for Isw2 alone (-) and in the presence of histone octamer (Oct), 601-50 DNA (DNA), 601-50 nucleosome (Nuc), and 601-50 nucleosome including a 10:1 molar ratio of ATP γ S to ATP (γ S). ATP hydrolysis by Isw2(K215R) was measured in the presence of 601-50 nucleosomes (K215R). Error bars correspond to 1 standard deviation. (C) Isw2/601-50 nucleosome complexes visualized by native gel electrophoresis. Components of each reaction are listed above the gel in order of addition (top to bottom) for lanes 2-7. Lanes M and 1 are 100 bp marker and 601-50 DNA, respectively. Band identities are indicated on the right.

Isw2/mononucleosome complex (Figure 1C, lane 3) that changes slightly in mobility upon addition of ATP (Figure 1C, lane 4). Identical reactions were carried out with the exception that plasmid DNA was added prior to loading to strip bound Isw2 from the mononucleosome template (Figure 1C, lanes 5-7). Addition of ATP (Figure 1C, lane 7) shifts the translational position of the nucleosome to a more central position, consistent with the outcome of Isw2 reactions on similar mononucleosome templates (Kassabov *et al*, 2002; Gaillard *et al*, 2003).

Nucleotide dependency of Isw2 binding to DNA

Isw2 was incubated with 2 M equivalents of 601-50 DNA and 1 mM of the indicated nucleotide, and the reaction products were immediately run on a native polyacrylamide gel (Figure 2A). Addition of Isw2 in the absence of nucleotides shifted the DNA into two slower migrating species (Figure 2A, lane 2). Higher ratios of remodeler to DNA resulted in an increase in the ratio of the upper to lower band, suggesting that the upper band is composed of two Isw2 complexes

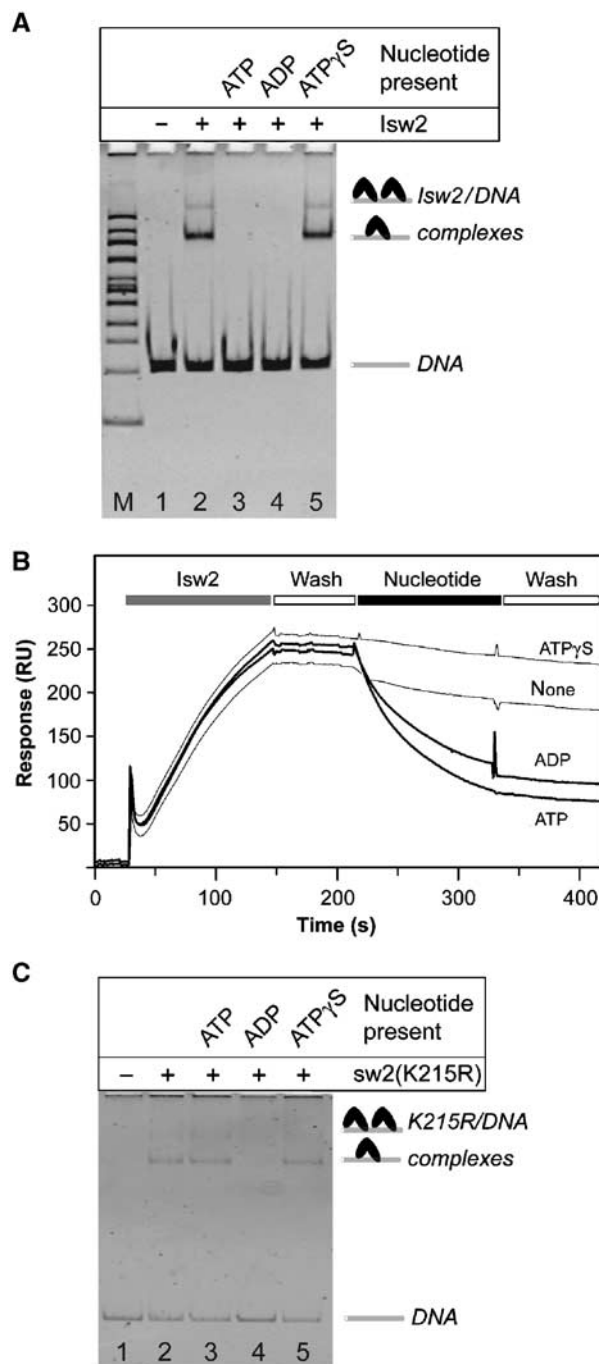


Figure 2 Isw2 binding to DNA is nucleotide dependent. (A) Native gel analysis of Isw2 binding to DNA. Isw2 was incubated with 2 M equivalents of 601-50 DNA and 1 mM of the indicated nucleotide (top) for lanes 2-5. Lanes M and 1 are 100 bp marker and 601-50 DNA, respectively. Band identities are indicated on the right. (B) Real-time Isw2/DNA binding studies. Representative SPR sensorgrams of four separate experiments are shown. Isw2 was passed over immobilized 601-50 DNA and followed with a wash solution. Isw2 dissociation was measured in the presence of the indicated nucleotides. (C) Native gel analysis of Isw2(K215R) binding to 601-50 DNA. Isw2(K215R) was incubated with 2 M equivalents of 601-50 DNA and 1 mM of the indicated nucleotide (top) for lanes 2-5. Lane 1 is 601-50 DNA. Band identities are indicated on the right.

bound per DNA. SDS gel analysis of the slower migrating species revealed that they contain both Isw2p and Itc1p (data not shown). Addition of either 1 mM ATP or ADP to the reaction abolished formation of the shifted products

(Figure 2A, lanes 3 and 4). In contrast, inclusion of ATP γ S (Figure 2A, lane 5) did not inhibit formation of the Isw2–DNA complex. The order of addition of protein, DNA, and nucleotide did not affect these reactions. Binding of Isw2 to circular or linearized plasmid DNA exhibited the same nucleotide dependency as was observed with linear 601-50 DNA (data not shown), ruling out any DNA-end effects as a cause for the observed nucleotide-dependent dissociation of Isw2 from DNA. Titration of Isw2 with ADP in the presence of DNA and quantification of the Isw2/DNA complex formed on native gels indicated that the K_i for ADP inhibition of DNA binding by Isw2 is approximately 100 μ M (data not shown).

The results presented in Figure 2A were confirmed by surface plasmon resonance (SPR) measurement using a BIAcore instrument. Real-time interaction assays were carried out under identical solution conditions in both the presence and absence of nucleotides. Isw2 protein and nucleotide solutions were passed over 700 resonance units of immobilized 601-50 DNA. Approximately 250 resonance units of Isw2 were loaded onto the DNA in the absence of nucleotides. Dissociation of protein from the DNA template was then monitored following injection of buffer containing ATP, ADP, or ATP γ S as indicated (Figure 2B). Inclusion of ATP γ S did not increase dissociation from the DNA. In contrast, injection of either ATP or ADP drastically affected Isw2 dissociation from the immobilized DNA template, with dissociation rates increasing over 10 times upon nucleotide addition. The dissociation rate constants for the Isw2/DNA complex without nucleotide and in the presence of ATP, ADP, and ATP γ S are $(1.2 \pm 0.2) \times 10^{-3}$, $(2.0 \pm 0.3) \times 10^{-2}$, $(1.3 \pm 0.3) \times 10^{-2}$, and $(8.7 \pm 1.5) \times 10^{-4} \text{ s}^{-1}$, respectively.

An Isw2 mutant defective in ATP hydrolysis permits ADP-induced DNA release

Isw2(K215R) was incubated with 2 M equivalents of 601-50 DNA and 1 mM of the indicated nucleotide, and the reaction products were immediately run on a native polyacrylamide gel (Figure 2C). Addition of the mutant Isw2 in the absence of nucleotides shifted the DNA into slower migrating species (Figure 2C, lane 2). In contrast to wild-type Isw2, the addition of ATP did not eliminate formation of the shifted products (Figure 2C, lane 3). As with wild-type Isw2, addition of ADP to the reaction abolished formation of the shifted products (Figure 2C, lane 4), and inclusion of ATP γ S (Figure 2C, lane 5) did not inhibit formation of the Isw2(K215R)/DNA complex.

Solution studies of Isw2 in the presence of nucleotides

We considered the possibility that the observed nucleotide dependency of Isw2 interaction with DNA was due to nucleotide-induced variation in protein stoichiometry. To address this possibility, Isw2 was analyzed by equilibrium analytical ultracentrifugation both in the presence and absence of nucleotides. In the absence of nucleotides, the apparent molecular mass of Isw2 was determined to be 271 ± 19 kDa. The presence of ADP (264 ± 12 kDa) or ATP γ S (263 ± 15 kDa) did not significantly alter the apparent molecular mass. Since the calculated molecular mass of the Isw2p–Itc1p heterodimer is 275 kDa, these results indicate that Isw2 remains a heterodimer irrespective of the state of nucleotide binding.

To investigate whether the conformational state of Isw2 is nucleotide dependent, velocity analytical ultracentrifugation

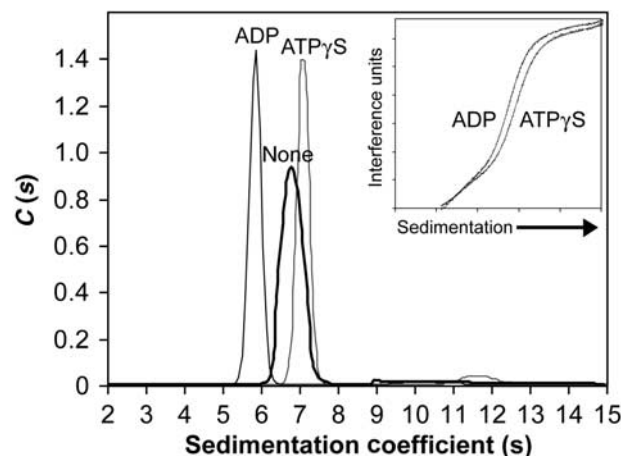


Figure 3 Sedimentation velocity analysis of Isw2 in the presence of nucleotides. Isw2 was sedimented alone (none) and in the presence of 1 mM ADP or ATP γ S. Representative s -value distributions are shown for each of the three conditions. The sedimentation boundaries shown for Isw2 correspond to centrifugation for 3 h in the presence of either 1 mM ADP or 1 mM ATP γ S. The predicted boundary shapes from the s -value distribution model are also shown and superimpose on the measured boundaries for both conditions (inset).

was performed both in the presence and absence of nucleotides. The s -value distribution observed in the absence of nucleotides, in the presence of ADP, and in the presence of ATP γ S revealed that each of the three Isw2 samples sediments predominantly as a single species but at different rates (Figure 3). The ADP-bound form of Isw2 sediments more slowly than the ATP γ S-bound form, whereas both the nucleotide-bound forms consistently displayed narrower s -value distributions than the nucleotide-free form. Since the results of equilibrium ultracentrifugation rule out the possibility of nucleotide-dependent variation in subunit stoichiometry, the observed differences in sedimentation rates indicate that Isw2 is significantly more compact in the presence of ATP γ S (7S) versus ADP (5.8S). Direct observation of sedimentation boundaries for Isw2 in the presence of these two nucleotides further demonstrates this point (Figure 3, inset).

Nucleotide dependency of Isw2 binding to 601-50 nucleosomes

The experiments shown in Figure 2A and B were repeated under identical solution conditions with 601-50 nucleosomes. Isw2 was incubated with 1.3 M equivalents of 601-50 nucleosomes and 1 mM of ATP, ADP, or ATP γ S. Following incubation, the products were run on a native polyacrylamide gel (Figure 4A). In the absence of nucleotides, addition of Isw2 shifted the nucleosome into a slower migrating species (Figure 4A, lane 3). Preparative electrophoresis demonstrated that this species contains each of the four core histone proteins, Isw2p and Itc1p (data not shown). The addition of ATP, ADP, or ATP γ S prior to loading did not significantly inhibit formation of the Isw2/mononucleosome complex (Figure 4A, lanes 3–6). Addition of ATP shifted the translational position of the nucleosome to a more central position (Figure 4A, lane 4). An identical experiment using tetranucleosome arrays (Schalch and Richmond, in preparation) also showed no nucleotide dependency for formation of Isw2/tetranucleosome complexes (Figure 4C).

The results of the Isw2–nucleosome binding experiments were confirmed by real-time SPR interaction assays. 601–50 DNA was biotinylated on the 601 terminus and used for mononucleosome assembly. The resulting nucleosome was indistinguishable from the unmodified nucleosome as judged by native gel electrophoresis and cleavage with MNase and DNase I (data not shown). Approximately 200 resonance units of Isw2 were loaded onto 4500 resonance units of immobilized mononucleosome and then washed with a solution containing the indicated nucleotide (Figure 4B). Injection of ATP γ S did not increase the dissociation rate relative to buffer solution alone. Injection of ADP or ATP resulted in a slight increase in dissociation rate from the mononucleosome template, but dissociation still occurred 20–30 times more slowly than from the naked DNA template. The dissociation rate constants for the Isw2/nucleosome complex without nucleotide and in the presence of ATP, ADP, and ATP γ S are $(7.5 \pm 1.5) \times 10^{-4}$, $(2.5 \pm 0.3) \times 10^{-3}$, $(1.6 \pm 0.3) \times 10^{-3}$, and $(9.5 \pm 1.2) \times 10^{-4} \text{ s}^{-1}$, respectively. Combined with less precise measurements for the association rate constants (data not shown), the dissociation rates measured here permit rough estimates for the equilibrium dissociation constants for Isw2 complexes. With the exception of Isw2/DNA complexes in the presence of ATP and ADP having K_D values greater than 1 mM, the K_D values of Isw2/DNA and Isw2/mononucleosome complexes in the presence of no nucleotide, ATP, ADP, and ATP γ S are all 1–10 nM.

Exonuclease III analysis of the Isw2/601–50 nucleosome complex

Although Isw2 remains bound to 601–50 nucleosomes throughout its ATP hydrolysis cycle, results of the Isw2/DNA binding studies suggest that changes in Isw2/DNA contacts should occur at the appropriate steps in the cycle. Therefore, uniquely end-labeled 601–50 nucleosome was bound to Isw2 under conditions in which they form a 1:1 complex (Figure 4A), and then probed with exonuclease III (Exo III) to visualize whether or not contacts between Isw2 and DNA flanking the nucleosome core change in the presence of nucleotides. Following Exo III digestion, the Isw2/mononucleosome complex remained intact as a 1:1 complex as observed by native gel electrophoresis (data not shown). A digestion time course of 601–50 nucleosomes in the absence of Isw2 revealed that Exo III digests the DNA flanking the nucleosome core largely without sequence preferential pausing, but comes to a stable halt at the 601 core DNA (Figure 5, lanes 1–4). In the presence of Isw2, cleavage is inhibited, leaving full-length DNA predominately and two minor fragments with termini 40 and 10 bp from the nucleosome core (Figure 5, lanes 8–10). The addition of ATP γ S (Figure 5, lanes 5–8) to the Isw2/601–50 nucleosome complex reduced the amount of undigested DNA relative to nucleotide-free reactions, but increased the levels of the two weaker fragments. Addition of ADP (Figure 5, lanes 11–13) resulted in a digestion pattern resembling that for the nucleosome in the absence of Isw2 (Figure 5, lanes 1–4).

Discussion

Chromatin remodeling complexes contain an ATPase domain that shares homology with members of the DEAD/H superfamily of DNA and RNA helicases (Gorbalenya and Koonin,

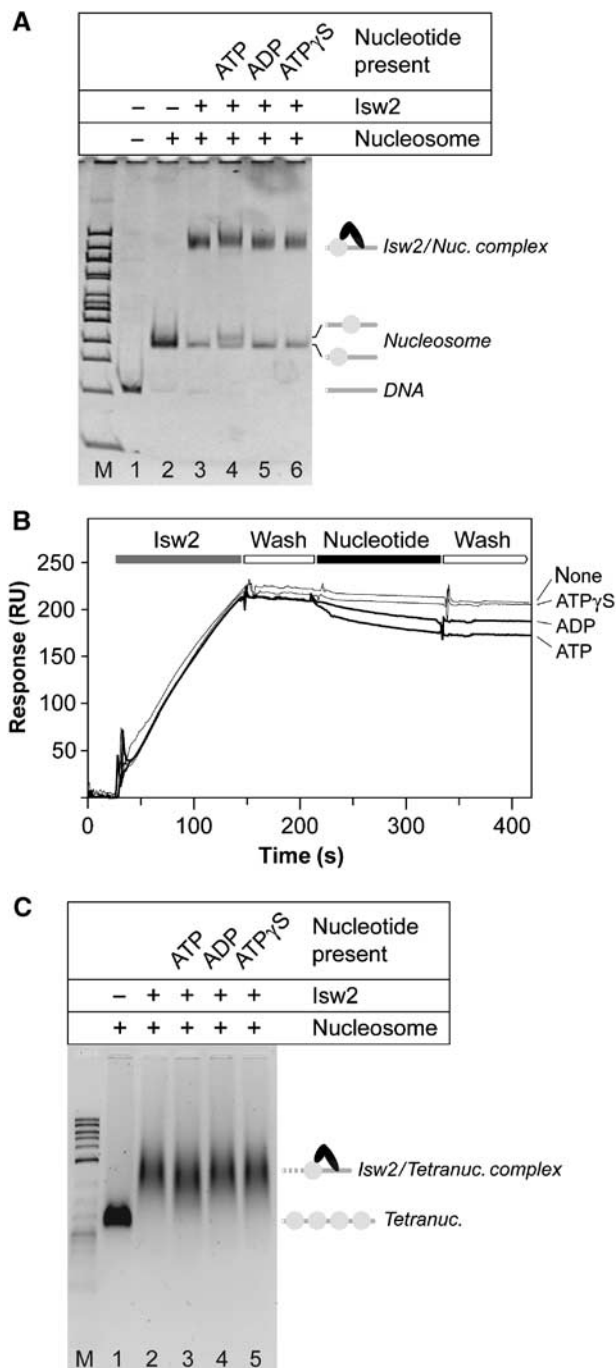


Figure 4 Nucleotide dependency of Isw2 binding to 601–50 nucleosomes. (A) Native gel analysis of Isw2 binding to mononucleosomes. Isw2 was incubated with 1.3M equivalents of 601–50 nucleosomes and 1 mM of the indicated nucleotides (top) for lanes 2–6. Lanes M and 1 are 100 bp marker and 601–50 DNA, respectively. Band identities are indicated on the right. (B) Real-time Isw2/mononucleosome binding studies. Isw2 was passed over immobilized 601–50 nucleosome and followed with a wash solution. Isw2 dissociation was measured in the presence of the indicated nucleotides. (C) Native agarose gel analysis of Isw2 binding to tetranucleosomes. Tetranucleosomes were incubated with 3.0M equivalents of Isw2 and 1 mM of the indicated nucleotides (top) for lanes 2–6. Lanes M and 1 are 2-log DNA marker and tetranucleosome, respectively. Band identities are indicated on the right.

1993). Helicase proteins separate regions of double-stranded polynucleic acid into their component single strands by combining a duplex destabilization reaction with DNA trans-

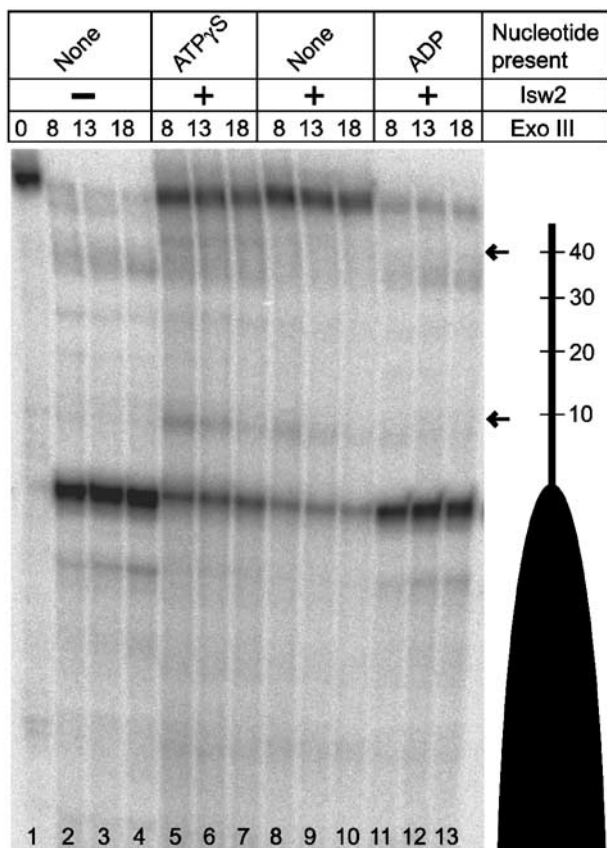


Figure 5 Exo III analysis of the Isw2/601-50 nucleosome complex. Isw2 was incubated with 1.0M equivalent 601-50 nucleosomes and 1 mM of the indicated nucleotides (top). Exo III digestion was allowed to proceed for the indicated times in minutes (top) at 32°C, and the samples were analyzed on a 6% denaturing gel. The 601-50 nucleosome is depicted schematically by a dark oval (right). The distance in base pairs along the DNA flanking the 601 nucleosome core is also indicated. Isw2-specific pauses are marked by arrows. Lane numbers are indicated (bottom).

location. In the case of the PcrA DNA helicase, mutant versions of the protein were made that are defective in the duplex destabilization reaction but continue to exhibit ATP-dependent DNA translocation (Soultanas *et al*, 2000). Similarly, separation of template binding, translocation, and duplex destabilization was demonstrated for the *Escherichia coli* Rho helicase (Walstrom *et al*, 1997). A chromatin remodeling complex that displays duplex destabilization activity has not been reported and until recently it was not clear what, if any, functional property remodeling factors might have in common with helicase proteins. However, new studies provide evidence that several chromatin remodeling factors, including members of the ISWI family, are ATP-dependent translocases (Fyodorov and Kadonaga, 2002; Saha *et al*, 2002; Whitehouse *et al*, 2003).

The ATP hydrolysis cycle of helicases drives an ordered program of alterations in protein conformation that defines the smallest repeating step of the overall strand separation reaction. Crystal structures of the PcrA helicase with and without a nonhydrolyzable ATP analog provide evidence that contacts between the γ -phosphate of ATP and highly conserved basic residues of a domain distinct from the nucleotide-binding domain are lost following ATP hydrolysis and

result in large-scale rearrangements in relative domain orientation (Velankar *et al*, 1999). In addition, structures of other helicase proteins in the absence of nucleotides reveal that analogous conformational changes might potentially be driven by nucleotide binding or hydrolysis (Korolev *et al*, 1997; Kim *et al*, 1998; Caruthers *et al*, 2000; Yamada *et al*, 2001). Structures of the T7 DNA helicase (Sawaya *et al*, 1999; Singleton *et al*, 2000) suggest that conformational changes induced by nucleotide cause this protein to display nucleotide-dependent DNA binding (Hingorani and Patel, 1993). Similarly, biochemical studies of numerous helicase proteins have shown that individual nucleotide-dependent conformations differ in their affinity for substrates (Wong and Lohman, 1992; Hingorani and Patel, 1993; Lohman and Bjornson, 1996; McDougal and Guarino, 2001; Henn *et al*, 2002; Majka and Burgers, 2003). The paradigm for nucleotide-dependent DNA binding is provided by recA, which has a structural architecture found in numerous helicase proteins (Bird *et al*, 1998). RecA's affinity for DNA is greatly increased in the presence of ATP γ S and decreased in the presence of ADP (Menetski and Kowalczykowski, 1985). A convincing explanation for this observation is provided by its crystal structure revealing that the sites of ATP binding/hydrolysis and DNA binding are juxtaposed and coordinated (Story and Steitz, 1992). In the case of chromatin remodeling complexes, the alternating binding and release of separate elements of the chromatin substrate during an ATP hydrolysis cycle is likely to define the component steps of the overall chromatin remodeling reaction.

In the present report, we demonstrate that the interaction between the yeast Isw2 chromatin remodeling complex and DNA is nucleotide dependent in the physiological salt range. Isw2 binds stably to naked DNA both in the absence of nucleotides and in the presence of a nonhydrolyzable ATP analog (Figure 2A and B). Conversely, both ATP and ADP were shown to promote dissociation of Isw2 from DNA (see Supplementary data provided, for a discussion of the result from an earlier study (Gelbart *et al*, 2001) on this point). The DNA binding displayed by both nucleotide-free and ATP analog-bound Isw2 suggests that loading onto DNA in the cell occurs readily both in the presence or absence of ATP. DNA binding studies using the ATPase-deficient Isw2(K215R) mutant support this view (Figure 2C). Since Isw2 hydrolyzes ATP to ADP when bound to DNA, the presence of ADP in the nucleotide-binding pocket appears to be responsible for the observed release of Isw2 from the DNA template. Results of analytical ultracentrifugation studies (Figure 3) revealed that Isw2 remains a heterodimer in the presence of nucleotides, but adopts a more compact conformation in the presence of ATP γ S than ADP. The combined results shown in Figures 2 and 3 indicate that DNA-binding domain(s) of Isw2 are physically linked to elements that undergo nucleotide-dependent conformational changes, and that the energy liberated by ATP hydrolysis is not required to drive their interconversion.

Isw2 binding to nucleosomes is absolutely dependent on DNA extending beyond the limits of the nucleosome core, and the ATPase activity of Isw2 increases as the length of flanking DNA increases (data not shown). These findings are consistent with previous studies showing that the ATPase and nucleosome-binding activities of *Drosophila* ISWI increase when a short length of DNA flanking the nucleosome core

is present, and suggest the presence of distinct nucleosome and flanking DNA-binding elements (Brehm *et al*, 2000; Whitehouse *et al*, 2003). More recently, elements of Isw2 have been shown to crosslink to flanking DNA (Kagalwala *et al*, 2004). Our interaction studies between Isw2 and 601-50 nucleosomes show that in solution conditions where both ATP and ADP induce Isw2 dissociation from DNA, Isw2 remains bound to the 601-50 nucleosome regardless of the nucleotide present (Figure 4). Exo III analysis of the Isw2/601-50 nucleosome complex revealed Isw2-dependent pausing of the nuclease on DNA flanking the 601 core, and that this pausing is nucleotide dependent (Figure 5). Consistent with the results of Isw2 binding to DNA (Figure 2), the presence of ADP decreased or eliminated Isw2-dependent Exo III pausing on DNA flanking the nucleosome core (Figure 5). Taken together, our results suggest that Isw2 DNA-binding elements gain and then lose hold of DNA in concert with each individual ATP hydrolysis event while separate nucleosome-binding elements maintain their grip.

We provide a model mechanism for Isw2 nucleosome remodeling combining the nucleotide dependency of Isw2 conformational states with the nucleotide dependency of its substrate interactions (Figure 6). On hydrolysis of ATP to ADP, Isw2 releases the flanking DNA from its 'DNA-binding site' and its conformation becomes extended (I-II), with rebinding to DNA facilitated by the release of ADP (II-III). ATP binding provides the energy to drive Isw2 compaction (III-IV). Persistence of the Isw2/flanking DNA interaction during compaction creates shearing and/or torsional stress between the histone octamer and associated DNA, which is relaxed by the histone octamer sliding along the DNA (IV-I). Sliding would occur in step lengths determined primarily by the extent of the ATP-driven conformational change of Isw2, but could also be influenced by the ability of a particular DNA sequence to reposition on the histone octamer. The nucleosome core is required for the stability of the Isw2/mononucleosome complex in the presence of ADP where flanking DNA would be unbound or weakly bound by Isw2.

A recent study utilized photocrosslinking to probe the Isw2-nucleosome architecture using a model mononucleo-

some nearly identical to that used in the present study (Kagalwala *et al*, 2004). Consistent with the results of our Exo III protection of the DNA flanking the nucleosome core (Figure 5), Kagalwala *et al* found an approximately 50 bp region of interaction between Isw2 and DNA immediately flanking the nucleosome core. A highly localized region of DNA contact within the nucleosome core accompanied the flanking DNA contact, demonstrating that specific interactions occur simultaneously within the nucleosome core and flanking DNA. The results of Kagalwala *et al* are well accommodated by our reaction cycle model (Figure 6).

The results presented here indicate that Isw2 would have near zero processivity on naked DNA and requires nucleosomes for translocation activity. The processivity value for the *Drosophila* ISWI protein estimated for nucleosome templates is 40 bp (Whitehouse *et al*, 2003). The triplex displacement experiments of Whitehouse *et al* (2003) shown in their Figures 4B and 5 indicate that zero or very limited processivity occurs for the naked DNA templates present in their samples. In contrast, the Snf2 family of remodeling complexes, which are distinct from the ISWI family, yield processivity values of 60–70 bp for naked DNA templates as determined in separate studies for yeast RSC, and for yeast SWI/SNF and RAD54p (Saha *et al*, 2002; Jaskelioff *et al*, 2003). Despite the analogy with DNA translocation by ATP-dependent DNA helicases, and that remodeling could occur via DNA translocation through a nucleosome in the manner suggested for RNA polymerase enzymes (Studitsky *et al*, 1997), our results indicate that Isw2 is better described as a nucleosome translocase. This view is consistent with the demonstration *in vivo* that Isw2-dependent chromatin remodeling is localized to a few nucleosomes in the promoters analyzed (Fazio and Tsukiyama, 2003), and suggests that dependencies on transcription factor and nucleosome interactions are important to gain and maintain template commitment.

Recent studies have revealed that *Saccharomyces cerevisiae* contains both a two-subunit complex comprising Isw2p and Itc1p, as studied here, and a second four-subunit complex additionally comprising the relatively small, histone fold containing proteins Dls1p and Dpb4p (Iida and Araki, 2004; McConnell *et al*, 2004). Although the presence of these subunits is not required for Isw2 interaction with chromatin as shown by CHIP assays (McConnell *et al*, 2004), determining their effect on translocation, if any, will be of interest.

Materials and methods

ISWI purification and preparation of samples for interaction assays

Recombinant Isw2 was expressed and purified as described (Gaillard *et al*, 2003). Following the final purification step, protein was immediately concentrated to 5–10 mg/ml using Vivaspin concentrators in 'remodeling buffer' solution (RB: 130 mM KCl, 1 mM MgCl₂, 1 mM DTT, 25 mM Tris-HCl, pH 7.3). PCR was used to create the Isw2(K215R) mutant using an oligonucleotide spanning both the K215 DNA and the *AvrII* restriction site in Isw2p, which is 24 bp 3' of the K215 codon (GenBank # CAA99622.1). Expression and purification of Isw2(K215R) was carried out as for wild-type Isw2.

All experiments were performed with Isw2 complex stored at 4°C for less than 8 h following the final purification and concentration steps. Proteins were diluted to the required concentrations in RB immediately before each measurement. Samples were monodisperse as judged by dynamic laser light scattering using a

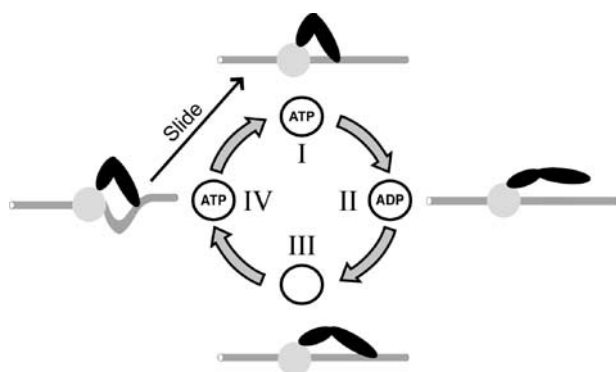


Figure 6 Model for coupling the Isw2 nucleosome remodeling reaction with an ATP hydrolysis cycle. The Isw2 complex (two black ovals) bound to a nucleosome (core: circle; flanking DNA: rod) is depicted in four states (I–IV), which represent differences in (1) Isw2 nucleotide binding, (2) Isw2 DNA binding, (3) Isw2 conformation, and (4) DNA position in the nucleosome core. The reaction cycle is described in the text. The depiction is not intended to suggest relative Isw2p and Itc1p subunit locations.

WyattQUELS System (Wyatt Technology). Further information on Isw2 handling and stability is presented in Supplementary data.

Histone purification and nucleosome assembly

Expression of *Xenopus laevis* core histone proteins, purification, and mononucleosome assembly were carried out as described (Luger *et al*, 1999).

601-50 DNA preparation

601-50 DNA was PCR amplified from a 601 clone (gift of J Widom) using primers 5'-CCCTCGAGGATATCGCCGCCTGGAGAATCCCGG and 5'-CCCGTACCGTTCGACGCCCAAGCTTGCATGCCTGCACATATCAGATCTTACATGCAC. A plasmid containing multiple copies of the 601-50 DNA was constructed using the *Sall* and *XhoI* sites in the primer sequences, and monomer 601-50 DNA was prepared by *EcoRV* digestion of the resulting plasmid.

ATPase assays

To compare directly the activity of recombinant Isw2 with the endogenous yeast complex, ATPase assays were performed as previously described (Tsukiyama *et al*, 1999). TLC reactions were visualized using a Fujifilm BAS-2500 Phosphorimager and quantified with Advanced Image Data Analyzer 2D v3.11 software (Raytest Isotopenperate GmbH).

Native gel interaction assays

In all, 100 μ l of 200 nM 601-50 DNA or 601-50 nucleosomes was prepared in RB with or without 1 μ l of 100 mM stock of ATP, ADP, or ATP γ S (Fluka) added. A 20 μ l portion of Isw2 diluted in RB (to 500 nM in Figure 2A, and to 770 nM in Figure 4A) was added and the reaction was allowed to proceed for 8 min at 32°C. Nucleosome remodeling reactions (Figure 1C) were performed in RB. For Figure 1C (lanes 5–7), samples were brought to a final concentration of 170 mM KCl following the reaction and a 10-fold molar excess of pUC19 plasmid DNA was added. Analysis by native polyacrylamide gel (4.5% acrylamide) electrophoresis was carried out at 4°C using ethidium bromide for visualization as described previously (Flaus *et al*, 1996). Analysis by native agarose gel (0.9% agarose, 45 mM Tris borate, 1 mM EDTA, pH 8.0) electrophoresis was performed at 4°C for 1.5 h at 50 V using ethidium bromide for visualization.

The binding of Isw2 to DNA is highly dependent on ionic strength. For example, the rate of dissociation of Isw2 from DNA in the absence of nucleotides increases with increasing monovalent salt, and at 190 mM KCl, is comparable to that seen with ADP or ATP at 130 mM KCl. Below 80 mM monovalent salt and in the range of 0–5 mM divalent ion, the Isw2/DNA complex has a dissociation half-life measured in hours. Therefore, experiments in this study were carried out at approximately physiological ionic strength (130 mM NaCl, 0–5 mM MgCl₂, 25 mM Tris-HCl, pH 7.3).

Real-time SPR (BIAcore) interaction assays

Real-time binding experiments were performed on a BIAcore 3000 biosensor system (Pharmacia Biosensor AB) at 22°C. A 100 μ l volume of 1 μ M 601-50 DNA was labeled with biotin-14-dCTP (Invitrogen) by incubation with Terminal Transferase (New England Biolabs) for 1 h at 30°C. Following incubation, the sample was dialyzed exhaustively against water. For preparation of 601-50 DNA, one biotinylated end was removed by *TaqI* (New England Biolabs) digestion, and the resulting DNA fragment was excised, purified from an agarose gel and used for nucleosome assembly. DNA or mononucleosomes were coupled to an SA biosensor chip (Amersham Pharmacia), and interaction studies performed with Isw2

protein in RB at a constant flow rate of 10 μ l/min. Injections were performed using the 'quickinject' setting. Between measurements, the sensor chip was regenerated at a flow rate of 100 μ l/min with 100 μ l RB at 900 mM KCl for DNA, or RB at 220 mM KCl for mononucleosomes. Mononucleosomes could also be regenerated at 155 mM KCl with the inclusion of 100 μ g/ml competitor DNA. With immobilized mononucleosomes, each sensor chip lane was used for only four measurements and the presence of histone proteins was confirmed following data collection by washing with 2 M KCl and monitoring loss of baseline signal. Individual binding curves were recorded four times. For both DNA and mononucleosome binding, Isw2 was loaded in RB at 110 mM KCl and dissociation was monitored in RB with and without nucleotides. Nonspecific binding of Isw2 to an uncoupled chip surface contributed less than 1% to the total signal under the described conditions. Data were processed using the BIAevaluation software package (Pharmacia Biosensor AB).

Analytical ultracentrifugation

Isw2 (2 μ M) was prepared in RB alone, with 1 mM ADP, and with 1 mM ATP γ S. Samples were centrifuged in an eight-hole rotor containing 12 mm double sector cells with sapphire windows in a Beckman XL-I analytical ultracentrifuge at 4°C. Partial specific volumes and solution density were calculated using Sednterp v1.08. Sedimentation equilibrium experiments were carried out at 9000, 12 000, and 14 000 rpm and interference data were analyzed using the global analysis component (one noninteracting species) of Ultrascan v6.0. The apparent molecular mass values reported (± 1 standard deviation) are the average of three measurements from three separate protein preparations. Four separate sedimentation velocity experiments were carried out under identical solution conditions as the equilibrium experiments at a speed of 30 000 r.p.m. Interference data were analyzed using continuous *c*(s) distribution of Sedfit v8.52b.

Exo III analysis of Isw2/601-50 nucleosome complexes

A 10 μ l portion of 1 μ M 601-50 DNA was 3' end labeled by incubation with terminal transferase (New England Biolabs) and ATP γ P32 for 1 h at 37°C, and then the label on one strand was removed by *TaqI* (New England Biolabs) digestion. The DNA fragment was purified by agarose gel electrophoresis, mixed with an excess of unlabeled DNA, and assembled into mononucleosomes. Isw2/601-50 nucleosome complexes were analyzed by Exo III in RB in the presence of 1 mM of the indicated nucleotides, and the samples were processed and analyzed as described (Fitzgerald and Anderson, 1998). Gels were calibrated by restriction digestion of the uniquely end-labeled 601-50 DNA.

Supplementary data

Supplementary data are available at *The EMBO Journal* Online.

Acknowledgements

We are grateful to Thomas Schalch for assistance with ultracentrifuge analysis, and to Ralf Wellinger and Kazuhiro Yamada for helpful discussions. DJF was supported by a Human Frontiers Science Program (HSFP) postdoctoral fellowship. IB was a recipient of a Liebig fellowship from the Fonds der Chemischen Industrie (FCI, Germany). We appreciate support from the Swiss National Fund through a grant to TJR and from membership in the NCCR Structural Biology.

References

- Becker PB, Hörz W (2002) ATP-dependent nucleosome remodeling. *Annu Rev Biochem* **71**: 247–273
- Bird LE, Subramanya HS, Wigley DB (1998) Helicases: a unifying structural theme? *Curr Opin Struct Biol* **8**: 14–18
- Brehm A, Langst G, Kehle J, Clapier CR, Imhof A, Eberharder A, Muller J, Becker PB (2000) dMi-2 and ISWI chromatin remodeling factors have distinct nucleosome binding and mobilization properties. *EMBO J* **19**: 4332–4341
- Caruthers JM, Johnson ER, McKay DB (2000) Crystal structure of yeast initiation factor 4A, a DEAD-box RNA helicase. *Proc Natl Acad Sci USA* **97**: 13080–13085
- Dorigo B, Schalch T, Bystricky K, Richmond TJ (2003) Chromatin fiber folding: requirement for the histone H4 N-terminal tail. *J Mol Biol* **327**: 85–96
- Fazzio TG, Tsukiyama T (2003) Chromatin remodeling *in vivo*: evidence for a nucleosome sliding mechanism. *Mol Cell* **12**: 1333–1340

- Fitzgerald DJ, Anderson JN (1998) Unique translational positioning of nucleosomes on synthetic DNAs. *Nucleic Acids Res* **26**: 2526–2535
- Flaus A, Luger K, Tan S, Richmond TJ (1996) Mapping nucleosome position at single base-pair resolution by using site-directed hydroxyl radicals. *Proc Natl Acad Sci USA* **93**: 1370–1375
- Flaus A, Owen-Hughes T (2001) Mechanisms for ATP-dependent chromatin remodelling. *Curr Opin Genet Dev* **11**: 148–154
- Fyodorov DV, Kadonaga JT (2002) Dynamics of ATP-dependent chromatin assembly by ACF. *Nature* **418**: 896–900
- Gaillard H, Fitzgerald DJ, Smith CL, Peterson CL, Richmond TJ, Thoma F (2003) Chromatin remodeling activities act on UV-damaged nucleosomes and modulate DNA damage accessibility to photolyase. *J Biol Chem* **278**: 17655–17663
- Gelbart ME, Rechsteiner T, Richmond TJ, Tsukiyama T (2001) Interactions of ISW2 chromatin remodeling complex with nucleosomal arrays: analyses using recombinant yeast histones and immobilized templates. *Mol Cell Biol* **21**: 2098–2106
- Gorbalenya AE, Koonin EV (1993) Helicases: amino acid sequence comparisons and structure–function relationships. *Curr Opin Struct Biol* **3**: 419–429
- Henn A, Shi S-P, Zarivach R, Ben-Zeev E, Sagi I (2002) The RNA helicase DbpA exhibits a markedly different conformation in the ADP-bound state when compared with the ATP- or RNA-bound states. *J Biol Chem* **277**: 46559–46565
- Hingorani MM, Patel SS (1993) Interactions of bacteriophage T7 DNA primase/helicase protein with single-stranded and double-stranded DNAs. *Biochemistry* **32**: 12478–12487
- Iida T, Araki H (2004) Noncompetitive counteractions of DNA polymerase epsilon and ISW2/yCHRAC for epigenetic inheritance of telomere position effect in *Saccharomyces cerevisiae*. *Mol Cell Biol* **24**: 217–227
- Jaskelioff M, Van Komen S, Krebs JE, Sung P, Peterson CL (2003) Rad54p is a chromatin remodeling enzyme required for heteroduplex DNA joint formation with chromatin. *J Biol Chem* **278**: 9212–9218
- Jenuwein T, Allis CD (2001) Translating the histone code. *Science* **293**: 1074–1080
- Kagalwala MN, Glaus BJ, Dang W, Zofall M, Bartholomew B (2004) Topography of the ISW2–nucleosome complex: insights into nucleosome spacing and chromatin remodeling. *EMBO J* **23**: 2092–2104
- Kassabov SR, Henry NM, Zofall M, Tsukiyama T, Bartholomew B (2002) High-resolution mapping of changes in histone–DNA contacts of nucleosomes remodeled by ISW2. *Mol Cell Biol* **22**: 7524–7534
- Kim JL, Morgenstern KA, Griffith JP, Dwyer MD, Thomson JA, Murcko MA, Lin C, Caron PR (1998) Hepatitis C virus NS3 RNA helicase domain with a bound oligonucleotide: the crystal structure provides insights into the mode of unwinding. *Structure* **6**: 89–100
- Korolev S, Hsieh J, Gauss GH, Lohman TM, Waksman G (1997) Major domain swiveling revealed by the crystal structures of complexes of *E. coli* Rep helicase bound to single-stranded DNA and ADP. *Cell* **90**: 635–647
- Lohman TM, Bjornson KP (1996) Mechanisms of helicase-catalyzed DNA unwinding. *Annu Rev Biochem* **65**: 169–214
- Luger K, Rechsteiner TJ, Richmond TJ (1999) Expression and purification of recombinant histones and nucleosome reconstitution. *Methods Mol Biol* **119**: 1–16
- Majka J, Burgers PMJ (2003) Yeast Rad17/Mec3/Ddc1: a sliding clamp for the DNA damage checkpoint. *Proc Natl Acad Sci USA* **100**: 2249–2254
- Marians KJ (2000) Crawling and wiggling on DNA: structural insights to the mechanism of DNA unwinding by helicases. *Structure* **8**: R227–R235
- McConnell AD, Gelbart ME, Tsukiyama T (2004) Histone fold protein Dls1p is required for Isw2-dependent chromatin remodeling *in vivo*. *Mol Cell Biol* **24**: 2605–2613
- McDougal VV, Guarino LA (2001) DNA and ATP binding activities of the baculovirus DNA helicase P143. *J Virol* **75**: 7206–7209
- Menetski JP, Kowalczykowski SC (1985) Interaction of recA protein with single-stranded DNA. Quantitative aspects of binding affinity modulation by nucleotide cofactors. *J Mol Biol* **181**: 281–295
- Saha A, Wittmeyer J, Cairns BR (2002) Chromatin remodeling by RSC involves ATP-dependent DNA translocation. *Genes Dev* **16**: 2120–2134
- Sawaya MR, Guo S, Tabor S, Richardson CC, Ellenberger T (1999) Crystal structure of the helicase domain from the replicative helicase-primase of bacteriophage T7. *Cell* **99**: 167–177
- Singleton MR, Sawaya MR, Ellenberger T, Wigley DB (2000) Crystal structure of T7 gene 4 ring helicase indicates a mechanism for sequential hydrolysis of nucleotides. *Cell* **101**: 589–600
- Soultanas P, Dillingham MS, Wiley P, Webb MR, Wigley DB (2000) Uncoupling DNA translocation and helicase activity in PcrA: direct evidence for an active mechanism. *EMBO J* **19**: 3799–3810
- Story RM, Steitz TA (1992) Structure of the recA protein–ADP complex. *Nature* **355**: 374–376
- Studitsky VM, Kassavetis GA, Geiduschek EP, Felsenfeld G (1997) Mechanism of transcription through the nucleosome by eukaryotic RNA polymerase. *Science* **278**: 1960–1963
- Thåström A, Lowary PT, Widlund HR, Cao H, Kubista M, Widom J (1999) Sequence motifs and free energies of selected natural and non-natural nucleosome positioning DNA sequences. *J Mol Biol* **288**: 213–229
- Tsukiyama T, Palmer J, Landel CC, Shiloach J, Wu C (1999) Characterization of the imitation switch subfamily of ATP-dependent chromatin-remodeling factors in *Saccharomyces cerevisiae*. *Genes Dev* **13**: 686–697
- Velankar SS, Soultanas P, Dillingham MS, Subramanya HS, Wigley DB (1999) Crystal structures of complexes of PcrA DNA helicase with a DNA substrate indicate an inchworm mechanism. *Cell* **97**: 75–84
- Walstrom KM, Dozono JM, von Hippel PH (1997) Kinetics of the RNA–DNA helicase activity of *Escherichia coli* transcription termination factor rho. 2. Processivity, ATP consumption, and RNA binding. *Biochemistry* **36**: 7993–8004
- Whitehouse I, Stockdale C, Flaus A, Szczelkun MD, Owen-Hughes T (2003) Evidence for DNA translocation by the ISWI chromatin-remodeling enzyme. *Mol Cell Biol* **23**: 1935–1945
- Wong I, Lohman TM (1992) Allosteric effects of nucleotide cofactors on *Escherichia coli* Rep helicase–DNA binding. *Science* **256**: 350–355
- Yamada K, Kunishima N, Mayanagi K, Ohnishi T, Nishino T, Iwasaki H, Shinagawa H, Morikawa K (2001) Crystal structure of the Holliday junction migration motor protein RuvB from *Thermus thermophilus* HB8. *Proc Natl Acad Sci USA* **98**: 1442–1447